Experimental Study of Reactive Chaotic Flows in Tubular Reactors

C. Boesinger, Y. Le Guer, and M. Mory
Laboratoire de Thermique Energétique et Procédés (LaTEP - EA 1932), Université de Pau et des Pays de l'Adour, (UPPA), rue Jules Ferry, 64 000 Pau, France

DOI 10.1002/aic.10455
Published online May 19, 2005 in Wiley InterScience (www.interscience.wiley.com).

For many reactive processes, fluid mixing has a significant effect on the rate of a chemical reaction and on the quality of the product. Mixing in a chaotic flow reactor is a promising phenomenon to control and optimize chemical processes. The effect of three-dimensional (3-D) chaotic flow advection on mixing efficiency and on chemical reaction advancement is examined. An experimental comparison is made, for low Reynolds number flows, between two tubular reactors made of successive bends, with the same number of bends (equal to 80) mounted in different configurations : a helical configuration (for regular flow) and a chaotic flow configuration with bends in perpendicular planes. We show that the mixing and the chemical reaction (for an instantaneous bimolecular chemical reaction) are more efficient in the chaotic flow reactor than in the helical reactor. The different effects of chaotic advection, molecular diffusion and reaction are discussed in view of laboratory findings. © 2005 American Institute of Chemical Engineers *AIChE J,* 51: 2122–2132, 2005

Introduction

The chaotic advection phenomenon has been used for now nearly 20 years to improve mixing (Ottino,[1] Aref,[2] for a historical review), and heat transfer (Peerhossaini et al.,[3] Mokrani et al.,[4] Acharya et al.[5]) within various closed or open flows. Within a deterministic laminar flow, particle trajectories can be chaotic since the equations for determining the particle's trajectories are in general not integrable. The result of chaotic advection is to create structured complex patterns with increasingly thin striations by the stretching and folding of the scalar field. In the early stages of the mixing process, the flow is primarily advective. This is called the stirring phase and the time evolution of the scalar field can be analyzed without taking diffusion into account. An example, shown in Figure 1, represents typical layered structures that can be observed in a cross-section of twisted pipes. When the scale of striations becomes sufficiently small, the molecular diffusion, which smoothes the gradients of the scalar, is fast enough to act in a dominating way. This is the mixing phase. Thus, the mixing problem, in terms of scalar homogenization, involves both the processes of advection and diffusion, the duration of which can vary considerably depending on the nature of the flow trajectories (regular, toroidal or chaotic). Mixing in turbulent flow has received much attention in the past, with the development of statistical approaches, but studies of chaotic flows show that mixing can also be efficient in a laminar flow, as pointed out by Alvarez et al.[6] Reactive chaotic flows are of major interest in the geophysical field (dynamics of the pollutants in the atmosphere or dynamics of biological populations in ocean currents), and in chemical engineering. Chaotic flows can be advantageously used in reactive processes for which fluid mixing has a significant effect on the rate of reaction and on the quality of the product (Zumbrunnen and Inamdar [7]). The considerable stretching of the intermaterial area between species can lead to effective mixing and fasten chemical reactions. However, in order to control the scales and spatial uniformity of the layered structures created by chaotic flows,[8,9] it is crucial to understand the interplay between chaotic advection and reaction in order to control and optimize chemical processes.

Correspondence concerning this article should be addressed to Y. Le Guer at yves.leguer@univ-pau.fr.

© 2005 American Institute of Chemical Engineers

Figure 1. Typical mixture plots obtained for a global chaotic flow stirring protocol at the exit of bends 8, 16 and 24, at a low Reynolds number in a twisted pipes mixer (numerical experiments by Le Guer and Schall, 2004).

The first plot corresponds to the inlet segregation state of the products.

The attention paid to the mixing mechanism in reactive chaotic flows is quite recent. Studies of reactive chaotic flows seem to have been reported for the first time by Ottino in his 1994 review article.[10] They concerned first the 1-D lamellar model, which gives some interesting results in agreement with experiments. However, this model fails to represent mixing processes on the large and small scales. In several 2-D studies, reactive mixing was approached first theoretically by considering the advection of discrete particles undergoing reactive collisions (Metcalfe and Ottino[11] in 1994 for the eccentric cylinder flow, Neufeld et al.[12] in 2000 for the sine flow, and in a compilation of previous studies, by Tél et al.[13] in 2000 for the Bénard-Von Karman wake downstream from a cylinder). Limitations of these studies were that either the diffusive mixing was ignored, a limited number of particles was considered, or a reduced region of the flow was examined. It is difficult to predict correctly the distribution of reactants and products since chaos produces high spatial heterogeneity in the concentration field. An improved approach to the modeling of a reactive sine flow was presented by Muzzio and Liu,[14] and Zalc and Muzzio,[15] when considering single bimolecular reactions, competitive-consecutive and parallel-competitive reactions. They showed that, for all cases considered, the outcome of the reactive system can be optimized by controlling the degree of chaos in the flow. The highest selectivities are always obtained for globally chaotic flows despite the persistence of spatial heterogeneities. A continuous spectral approach was adopted by Adrover et al.[16] for a bimolecular reaction in sine flow and cavity flow. They succeeded in developing a method which overcomes the problems related to numerical diffusion occurring for high Péclet numbers. This allows one to study how the reactive processes are affected by the existence of complex partially mixed structures, before they are completely mixed by diffusion. All experiments mentioned previously were performed for highly idealized flows in two-dimensions, in which the spatiotemporal evolution of reactive scalars is governed by advection-diffusion-reaction equations. Two types of 3-D flows have also been considered: closed flows, such those encountered in stirred tanks, and open flows, like those found in tubular reactors. Bryden and Brenner[17] studied numerically the transverse mixing between the eccentric cylinders in the presence of an axial flow. The reaction takes place at the surface of the outer cylinder. The reaction speed is multiplied by a factor of five for slow diffusive reactive species. Moreover, with the increase of transverse mixing, a reduction in axial dispersion is observed. For steady chaotic flows in tubular reactors with a fast bimolecular reaction, Tang and Boozer[18] established design criteria based on a local Lyapunov exponent analysis to predict the minimum length of the reactor for a desired "quality factor". This length varies logarithmically with the diffusivity of species. For reactive mixing in a stirring tank Lamberto et al.[19] used a neutralization reaction to determine the size and location of segregated regions. More recently, Szalai et al.[20] found that the statistical properties of the 3-D reactive flow are identical to those of 2-D reactive chaotic flow. Namely, the stretching is a self-similar process which controls the location and density of the intermaterial area between reactive components, and, consequently, controls the product concentrations.

Sawyers et al.[21] investigated numerically, from asymptotic approximations, the yield of a bimolecular reaction between two initially segregated reactants in a tubular reactor with different coiling geometries. They concluded that, whatever the reaction speed, the exponential stretching of the interface length between the two reactants for the "twisted Dean flow model" generates an increase in the mass fraction of the product. The geometry considered by Sawyers et al. is close to that considered in this study.

This review of previous studies reveal that most of the work done has been based on theoretical and numerical approaches. The only experimental work was performed for a 2-D flow by Paireau and Tabeling.[22] They studied the effect of mixing, in the unsteady-chaotic flow produced by two alternated corotating vortices, on the kinetics of a second-order reaction. As observed in numerical studies, they highlighted the major role played by persistent concentration gradients (filaments) in the improvement of global reactivity. This induces a dynamical catalytic effect.

This study is primarily motivated by the objective of considering in the laboratory some of the conclusions mentioned previously. By comparing different situations the aim is to observe that a reactive chaotic flow can enhance chemical reaction as compared to a non-chaotic flow having similar global properties. The experimental device is a tubular reactor composed of curved channels having their planes of curvature successively rotated by 90 °. We call this flow the *twisted Dean flow*. Between two successive bends, the contrarotating helical swirling cells (Dean cells) on both sides of the plane of curvature of a given bend are submitted to a reorientation of their symmetry axis. The performances of this chaotic flow reactor are compared with those obtained from a more classical helical reactor in which the flow is not chaotic. To our knowledge, our work is the first experimental reactive chaotic flow mixing study performed in a 3-D tubular open flow.

In the second section we describe the experimental setup. The third section focuses on the experimental techniques used in the mixing study, with and without chemical reaction. The next section presents the results obtained for nonreactive and reactive mixing in the chaotic flow reactor, and in the helical reactor for different flow rates. Conclusions and perspectives are addressed in the final section.

Experimental Setup

Reactors

Figure 2 shows a general picture of the experimental setup. Its consists of two different tubular reactors in parallel which can be used alternatively. The section of the reactors is circular

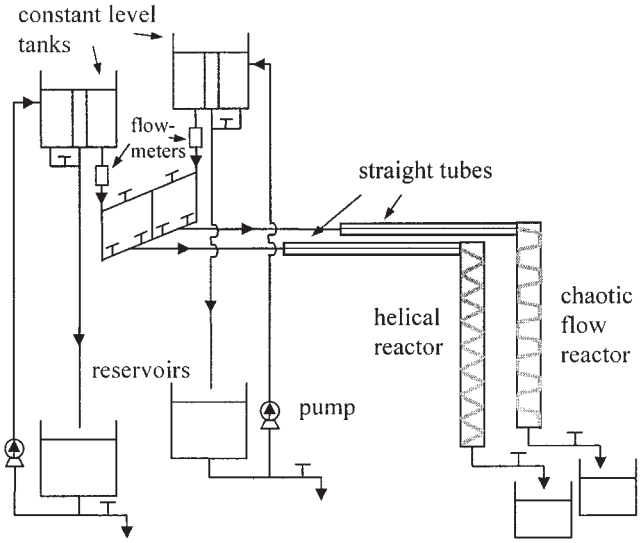

Figure 2. Helical and chaotic flow reactors.

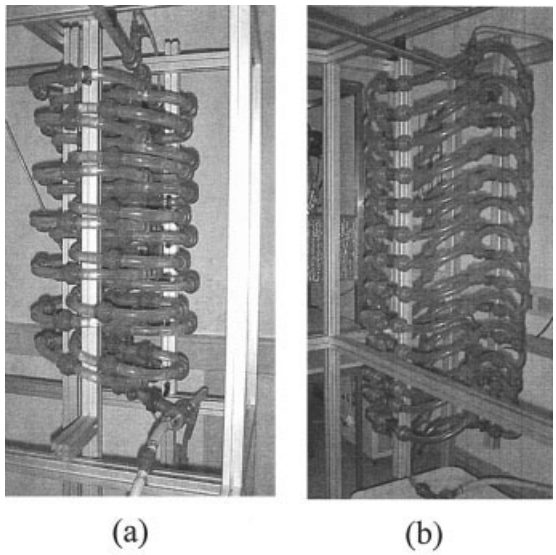

Figure 3. Reactors: (a) helical reactor, and (b) chaotic flow reactor.

and its interior diameter is $a = 20$ mm. The solutions to be mixed inside the reactors are introduced from two constantly level tanks (with an overflow system) on top of the installation, which contains 58.4 L each. Two pumps continuously maintain a constant level in the tanks from the reservoirs located underneath them. The water level in the tank exert constant pressure at the inlet of the reactors. The pressure drop across the reactors is maintained constant by gravity. The flow in the reactors is an open flow. The mixed solution is collected in a downstream reservoir at the outlets of the tubular reactors, where the pressure is the atmospheric pressure. Two rotameters at the entrance of the reactors allow us to measure and adjust flow rates with a maximum flow rate of 100 L/h.

Each tubular reactor is made up of two parts: an entrance test section and the coiled pipes. The constant level tanks are first connected to a straight tube divided into two semicircular channels by a plate coinciding with the tube's diameter. The length of this tube is 1.5 m. The thickness of the separating plate is 1 mm. This arrangement is designed to establish the flow of the two solutions in their respective semicircular channels, before they come in contact. The mixing and the reaction of the two solutions occur in the second part of the tubular reactors, which are made of 80 bends. Each bend produces a 90° rotation of the flow direction. The average radius of curvature is $R = 122 \pm 2{,}5$ mm ($a/R = 0{,}08 \ll 1$). Each bend is prolonged at both ends by short sections of straight tube. The average length of each element is 245 mm. The total length of each reactor is $L_t = 22{,}4$ m, and their volume is 7 L. The two reactors, which are shown in Figure 3, differ only in the arrangement of the successive bends:

- In the first reactor the bends are bound together to form a helix. The helix step is of the same dimension as the tube's diameter, so that all the bends are layed out in planes that are almost parallel. This reactor is called *helical reactor*. Figure 4a displays of two successive bends of the helical reactor. The position of a point in a curved tube section is given in the local (O,x,y) coordinate system with the Ox axis directed toward the center of the curvature of the bend. The "undeformed" secondary flows, in the form of Dean cells, generated inside the bends, are in Figure 4a. The Ox axis of the first bend of the reactor coincides with the separation plate in the upstream straight tube. Consequently, the interface between the two solutions is scarcely distorted by the secondary flows in the helix reactor. Secondary flows recirculate the fluid along the walls and the separatrix between the two cells, so that particles in the two solutions only come into contact during the diffusion process in the transversal Oy direction.
- As shown in Figure 3b, successive bends are in perpendicular planes in the second reactor. The rotation between the two successive bends is in the opposite direction of rotation than that between the two former bends. The second reactor, called a chaotic flow reactor, repeats the arrangement of six

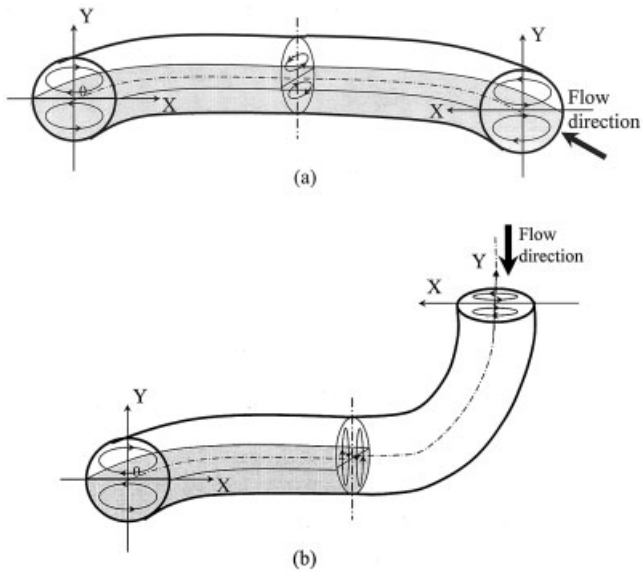

Figure 4. Direction of conductivity profile measurements: (a) helical reactor, and (b) chaotic flow reactor.

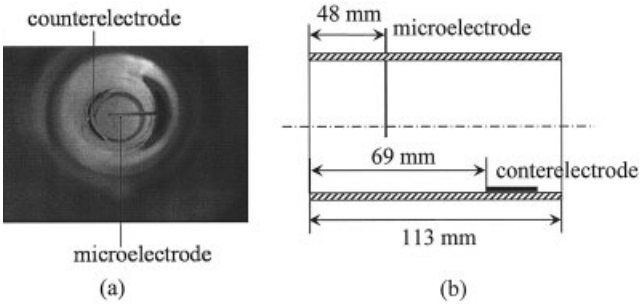

Figure 5. Conductivity probe: (a) photography in the cross-section plane, and (b) representation in the longitudinal cut-view.

successive bends. The shift angles between the bends are fixed at: +90°, −90°, +90°, −90°, +90°, and −90°, respectively. This configuration has the advantage of forming a pseudo-horled helix reactor, if short and straight pipe elements are inserted between every other three bends. It is generally accepted that the secondary flows are progressively modified in the stream's direction inside each new bend (Le Guer and Peerhossaini[23]). Figure 4b shows how the Dean cells' secondary currents stir the two solutions. As the separatrix between the two Dean cells is parallel to the separation plate of the upstream straight pipe, the stretching and folding of the interface starts only in the second bend. It is shown elsewhere (Le Guer et al.[24]) that the protocol of rotation (+90°, −90°, +90°, −90°, +90°, −90°) chosen for the chaotic flow reactor promotes stirring, as compared to the protocol of rotation (+90°, +90°, +90°, +90°, +90°, +90°). For the latter protocol, the secondary flows in a given bend partially compensate for the stirring produced in the preceding bend. This description simply explains that approriate rotation of the successive bends is necessary to increase stirring. On the other hand, the purpose of this article is neither to show that particle trajectories are chaotic, nor is it to find the best stirring protocol. We refer to Jones et al.[25] for a demonstration of the properties of chaotic trajectories. The problem of optimization of mixing by way of optimal stirring protocol was addressed in another study (Gibout et al.[26]).

For the implemention of conductimetric and sampling techniques, described in the two following sections, short straight tubes of 113 mm in length are inserted all the three bends. We call them "measurement modules". 25 measurement modules are included in each reactor.

Conductimetric method for measuring passive mixing

Mixing experiments of a solution of potassium chlorate KCl with clear water were conducted in the two reactors. They are designated as passive mixing experiments, as the constituents do not react together. The determination of the KCl concentration at different locations inside the reactor provides a quantitative estimate of mixing. It was measured using a conductimetric technique. This technique provides the local conductivity measurement of an electrolyte without perturbing the flow. For the purpose of our experiment, we refer to the former work of Manning and Wilhelm,[27] and Gibson and Schwarz,[28] for the design of a specific microelectrode. This microprobe (shown in Figure 5a) is made of a 50 mm long platinum wire of 0.6 mm in external dia. It is isolated by a heat-shrinkable sleeve, except at its end. The section at the end of the platinum wire, covered with black of platinum, is the sensitive element that measures the conductivity in its vicinity. The other end of the platinum wire is fixed to the piston of a syringe and connected by a tin-brazing to an electric wire. The movement of the syringe piston allows one to move the tip of the microelectrode across the internal diameter of the tubular reactors. The counter-electrode is a sheet of Nickel (200 mm^2 in surface) lying on the interior surface of the tubular reactor. A layout of the arrangement of the microelectrode, and of the counterelectrode in the reactor is shown in Figure 5b.

The theory of the conductimetric technique by Gibson and Schwarz shows that the surface of the counterelectrode has to be much larger than that of the sensitive element of the microprobe, and the size of the measurement volume must be small enough. Since this theory is established for a spherical microprobe, a specific procedure was defined in the course of our study for the calibration of the microprobe system. This procedure establishes that the size of the measurement volume, in which the sensor measures the averaged conductivity, is less than 1 mm. This work is described in more detail elsewhere (Boesinger[29]).

Sampling procedure for measuring mixing and chemical reaction advancement

The advancement of mixing and chemical reaction was quantitatively determined from the dosage of samples taken at different positions across the internal diameter of the tubular reactors. The chemical reaction considered and the dosage procedure are described in the next section. The next section also considers how transversal profiles of reagent concentrations can account for the general processes of mixing and reaction.

A hollow metal tube of 2 mm in internal diameter, which can be moved along diameters inside the tubular reactors, is used to take samples at different positions. The tube is bent at its end and aligned with the flow direction, and it is lengthened by a needle of 0.3 mm in internal diameter. The procedure of sampling was adjusted in order to suck in layers having a thickness of the same size as that of the needle's diameter, without disturbing the flow around it. This is obtained by adjusting the velocity of suction in accordance with the flow velocity at the position of sampling. It was previously verified, through flow visualizations, that the procedure of suction does not disturb the flow. The collected samples had a volume of 10 mL, and were homogenized by the use of a magnetic stirrer. The reaction is, therefore, complete before the dosage of samples are achieved. This does not exactly account for the level of mixing and the reaction advancement, which is actually achieved at the position of sampling and at the time the sample is taken. However, we estimate that the amount of time required for homogenizing by diffusion, of a layer of thickness of $\delta = 0.3$ mm, to be at the most $\delta^2/4D \approx 22$ s for a diffusivity of $D = 10^{-9}$ m^2/s. The time required to homogenize this sample layer inside the reactor corresponds to a downstream movement of the sampling position, which is less than the length of three bends. The variations of the mixing level in the sample, therefore, cannot cast doubt on the conclusions drawn in this article.

Table 1. Axial Positions of Measurement of Conductivity

Module Number	Number of Bends	L (m)	L/L_t
4	10	2.83	0.13
6	16	4.53	0.20
8	22	6.22	0.28
14	40	11.31	0.51
18	52	14.71	0.66
19	55	15.56	0.70
26	76	21.48	0.96

Experimental Study of the Transversal Mixing

Passive mixing experiments

Inlet hydrodynamic conditions. The mixing of nonreacting solutions along the helical and along the chaotic flow reactors have been compared for the same inlet conditions using the conductrimetric technique. Conductivity measurements were carried out in steady flow conditions. For the two reactors, the plane of curvature of the first bend is parallel to the plate separating the two solutions in the inlet's straight tube, allowing one to meet the same hydrodynamic conditions in the first bend of each reactor when the flow rates are the same. The separating plate inside the inlet tube is horizontal. Clear water is injected above it, whereas the solution with KCl is injected in the lower channel. We checked that the added quantity of KCl did not modify the density of water (1,000 kg/m^3). It is supposed that viscosity remains similar to that of water.

Transversal conductivity profiles

The evolution of KCl concentration distributions in different sections at the same distances from the inlet sections in the two reactors were compared for different flow rates. As the conductimetric technique provides a local measurement of the concentration of KCl in a measurement volume of a typical size of 1 mm, the variations of conductivity were only measured along the transversal direction by displacing the microelectrode along the Oy axis indicated in Figure 4. Measurements were carried out for the two reactors and compared for four flow rates. For the obtained data, the measurement modules were positioned downstream of bend numbers 10, 22, 40 and 76. Additional measurements were performed in the chaotic flow reactor downstream of bend numbers 16, 52 and 55, in order to determine more precisely the axial position, where the conductivity becomes homogeneous. Table 1 summarizes the different axial positions along the reactors, where the transversal conductivity profile are measured. The different hydrodynamic conditions investigated are reported in Table 2. The total flow rate Q is equal to the sum of the flow rates of the two solutions. The velocity U is the flow rate velocity.

In the helical reactor, the interface which initially separates the two solutions is not distorted by the secondary flows, and the evolution of the transversal conductivity profile is characteristic of the diffusion process of KCl across this interface. In the chaotic flow reactor, the measurement of transversal conductivity profiles in the Oy direction does not fully display the folding up of the interface which separates the two solutions in a given section. To see it, the conductivity should be measured over the entire section, using a microelectrode having a resolution lengthscale much smaller than 1 mm (in order to provide a view of the stirring process), and having a spatial resolution comparable to that of numerical experiments (see Figure 1). However, the differences in the evolution of the transversal conductivity profiles measured in the successive sections of the two reactors, are of such importance that they allow one to conclude, qualitatively and quantitatively, on the efficiency of mixing in the two reactors.

The different fluids used in our experiments had a temperature equal to 21 ± 1°C. The conductivity of clear water in the reservoir was 0.44 mS/cm and the conductivity of the initial KCl solution was 3.7 mS/cm for a KCl concentration of 3.1 10^{-2} mol/L.

Mixing with Chemical Reaction

Chemical reaction and inlet conditions

The mixing and the oxydoreduction reaction between the ion triiodide I_3^-, and the ion thiosulfate $S_2O_3^{2-}$

$$I_3^- + 2S_2O_3^{2-} \rightarrow 3I^- + S_4O_6^{2-} \quad (1)$$

were achieved in the two reactors and the results were compared. The ion triiodide is produced by the instantaneous reaction of iodine I_2, with ion iodide I^-, produced from potassium iodite.

$$I_2 + I^- \leftrightarrow I_3^- \quad (2)$$

The two reagents were prepared and diluted separately in the two tanks. The initial concentrations were $[I_3^-]_o = 5 \cdot 10^{-4}$, mol/L and $[S_2O_3^{2-}]_o = 1 \cdot 10^{-3}$ mol/L, so that the two reagents enter the reactors in stoechiometric proportion. Under these conditions, the reaction of triiodide with thiosulfate is a quasi-instantaneous reaction. The reaction (1) is a first-order reaction with respect to the two reagent concentrations with the chemical constant estimated to be $k = 1.29\ 10^6$ L mol^{-1} s^{-1} (Scheper and Margerum[30]), so that the characteristic time of reaction is $\tau_c = 1/k\lfloor S_2O_3^{2-} \rfloor_o = 7.810^{-4}$ s. The reaction speed implies that the achieved rate of conversion of the reagents inside the tubular reactors will depend mainly on the efficiency of the mixing between the reagents. The diffusivity of the reagents in water are $D_{I_3^-} = 2.10^{-9}$ m^2/s and $D_{S_2O_3^{2-}} = 1.10^{-9}$ m^2/s (Lide[31]). The diffusion time-scale of the reagents $\tau_D = \ell^2/D$ is less than the characteristic time of reaction τ_c only when the typical length scale of concentration gradients ℓ is less than 0.9 μm. Ion triiodide and ion thiosulfate, hence, cannot coexist. They undergo a chemical reaction as soon and they are in contact. Further advancement of the reaction relies on the subsequent advection and diffusion of the reagents.

For the small concentrations of reagents used in our exper-

Table 2. Parameters Relating to the Various Experiments Carried Out

Flow Q (ml/s)	Mean Velocity U (cm/s)	Reynolds Number $\mathrm{Re} = U \cdot 2a/\nu$	Dean Number $\mathrm{Dn} = \mathrm{Re} \cdot (a/R)^{1/2}$
2.63	0.84	167.5	48
5.26	1.68	335	96
10.52	3.36	670	192
15.78	5.04	1005	288

iments, temperature variations due to the chemical reaction were negligible and, therefore, the density of the solutions did not vary sufficiently enough from the density of clear water to produce flow disturbances. The inlet hydrodynamic conditions for the experiments with chemical reactions were the same as those for the passive mixing experiments. The triiodide solution and the thiosulfate solution were injected into the lower and into the upper channels of the inlet straight section of the reactors, respectively.

Transversal profiles of concentration

The advancement of the mixing and of the chemical reaction in the two reactors were studied in the same manner as done for the passive mixing experiments, except that the transversal profiles measured along the Oy direction are concentration profiles of ion triiodide and ion thiosulfate. The concentrations were measured from the dosage of samples taken using the sampling method described previously. All concentration profiles were determined from samples taken every 2 mm along the Oy axis, once the steady flow state was reached.

For the chaotic flow reactor the transversal concentration profiles were measured in the measurement modules downstream of bends 10, 16, 22, 55 and 76 (see Table 1), whereas they were only determined downstream of bend 76 for the helical reactor. This appeared to be sufficient to compare the efficiency of the mixing in the two reactors. Indeed, the mixture was not yet homogeneous at the outlet of the helical reactor. The flow conditions investigated in the experiments were the same in both types of experiments: those with and without reaction. The Reynolds numbers tested were Re = 335, 670 and 1005 (see Table 2).

As opposed to the brown coloring of triiodide, thiosulfate and ion iodide are transparent, allowing a qualitative monitoring of the progressive mixing and reaction in the reactors. This property is also used for the dosage of reagents in samples. Since the reagents cannot coexist in homogeneous samples after a duration of a few ms, the brown color of a sample indicates the presence of triiodide and the absence of thiosulfate. The dosage of the remaining triiodide is performed by adding thiosulfate until the solution becomes transparent. The opposite procedure is used when the sample is transparent: ion triiodide is added until a brown color appears.

Results

Passive mixing experiments

Figure 6 compares the evolution of the transversal conductivity profiles along the helical and chaotic flow reactors for a Reynolds number equal to 335. A qualitative analysis of the graphs obviously shows that the mixing process is more efficient in the chaotic flow reactor than in the helical reactor. The conductivity is homogeneous in the section of the chaotic flow reactor following bend 76, whereas complete mixing is far from being obtained in the helical reactor at the same position. Figure 7 shows the transversal conductivity profiles in the chaotic flow reactor downstream of bends 52, and 55 for the same Reynolds number. The mixture is homogeneous downstream of bend 55, whereas the solution is not yet homogeneous at the outlet of the helical reactor.

Figure 8 displays the evolution of the transversal profile of

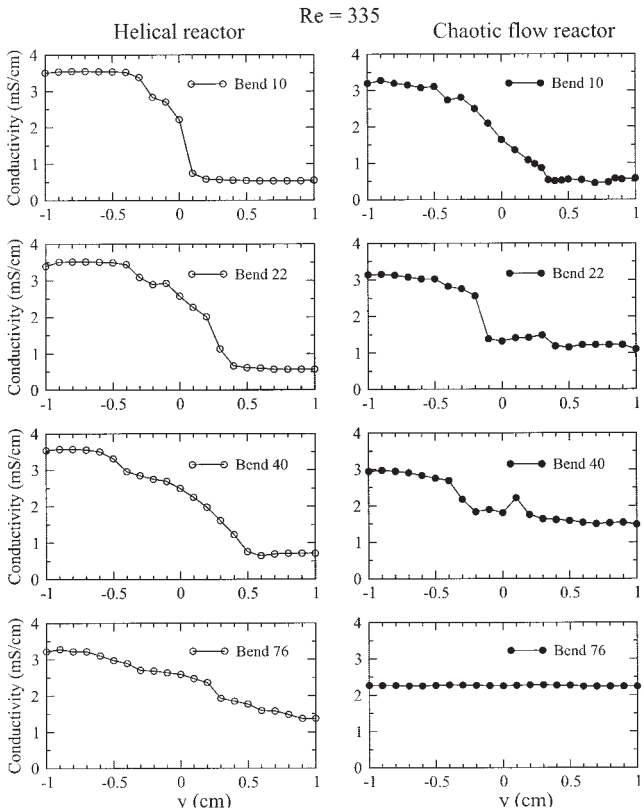

Figure 6. Evolution of transversal conductivity profiles at different axial positions along the helical and chaotic flow reactors for a Reynolds number Re = 335.

conductivity along the two reactors for four different Reynolds numbers ranging from 167.5 to 1005. A highly significant effect of the Reynolds number on the achievement of mixing is observed in the chaotic flow reactor. When the Reynolds number is over 670, the conductivity is homogeneous downstream of bend 22. The influence of the Reynolds number on the mixing seems much less significant in the helical reactor. This observation will be discussed further in the text.

Mixing efficiency

In order to quantify the efficiency of the mixing, we computed the standard deviation σ of conductivity from a homogeneous solution for the different transversal conductivity profiles

$$\sigma = \sqrt{\frac{1}{n}\sum_{i=1}^{n}\left(\frac{\gamma_i - \gamma_{moy}}{\gamma_{moy}}\right)^2} \tag{3}$$

n is the number of conductivity data measured in a profile, and γ_{moy} is the conductivity of the homogeneous mixture, corresponding to the average value of the conductivity profile (equal here to 2.25 mS/cm). When the standard deviation is less than 0.05, one can reasonably consider that the mixture is homogeneous in the section of the reactor. This value is actually

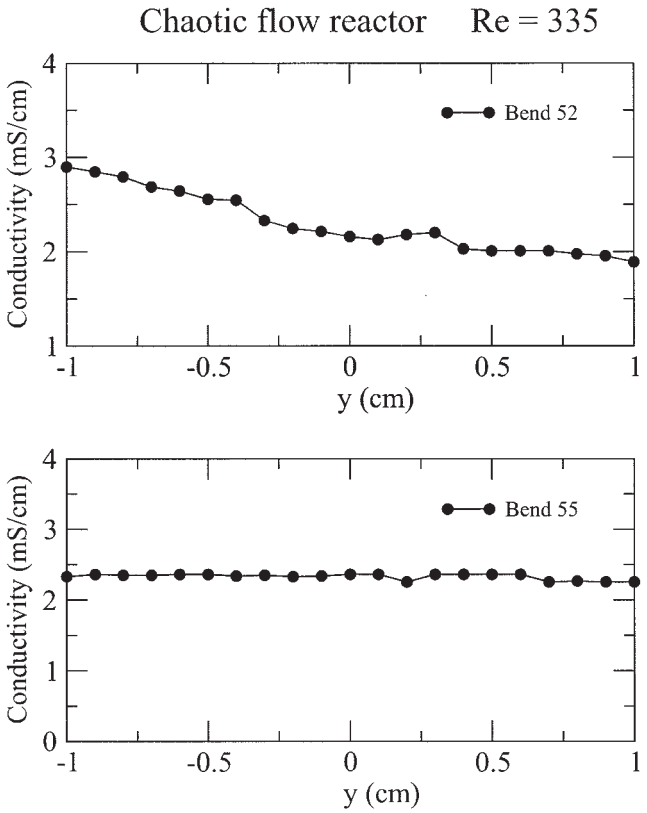

Figure 7. Evolution of transversal conductivity profiles along the chaotic flow reactor for a Reynolds number Re = 335.

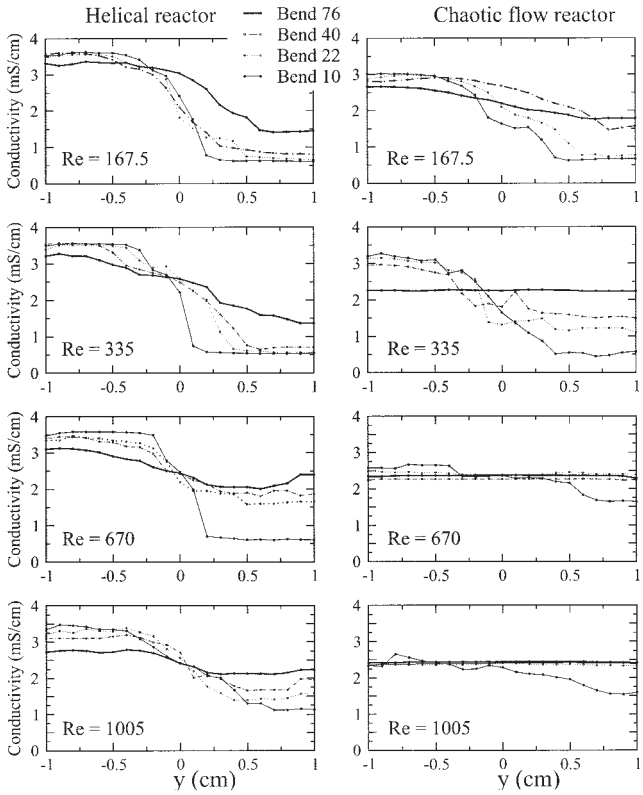

Figure 8. Evolution of transversal conductivity profiles for different axial positions along the helical and chaotic flow reactors.

obtained for the profile shown in Figure 7 downstream of bend 55.

Figure 9 shows the evolution of the standard deviation along the helical and the chaotic flow reactors for $Re = 335$, 670 and 1005. The quantity σ is plotted as a function of the dimensionless distance $z = L/L_t$. L is the distance where the profile is measured from the reactor inlet, and L_t is the total length of the reactor. As observed in Figure 9, the standard deviation decreases linearly as the distance increases. For $Re = 335$, the dimensionless rates of decrease of σ with the distance from the inlet being 0.918 and 0.397 for the chaotic flow reactor and the helical reactor, respectively. The evolution toward a fully mixed state is, therefore, 2.3 times faster in the chaotic flow reactor than in the helical reactor. An estimate of the length for mixing L^* is deduced from Figure 9, defined as the length where the standard deviation reaches the value $\sigma = 0.05$ (for $Re = 335$, this corresponds to the position downstream of bend 55). Table 3 summarizes the variations of L^*/L_t in the two reactors with the Reynolds number. The significant differences obtained in the chaotic flow reactor, and the helical reactor highlight the efficiency of mixing produced by chaotic advection. We also observe that the efficiency of mixing in the chaotic flow reactor is much enhanced when the Reynolds number increases. The stirring of fluid particles by the Dean cell's secondary flows, which change directions in the chaotic flow reactor when the plane of curvature of the bends rotate, is more efficient when the mean flow velocity is increased.

We notice from the data in Table 3 that the efficiency of mixing is also enhanced in the helical reactor by increasing the Reynolds number, although to a lesser extent as compared to the chaotic flow reactor. In the helical reactor, the mixing results from the process of diffusion across the interface of the plane Oxz, but we also observe a convection-enhanced trans-

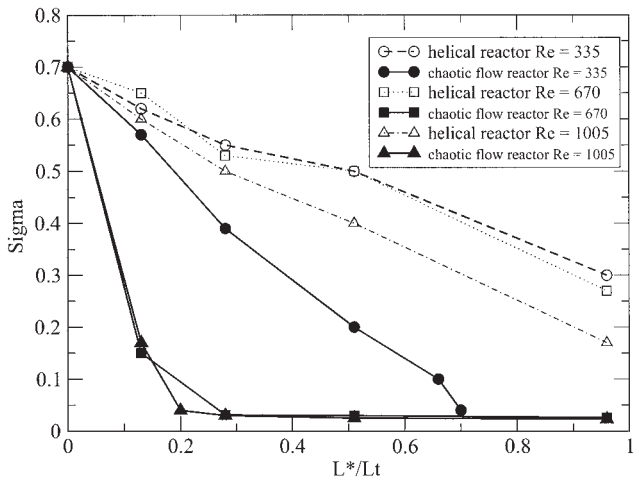

Figure 9. Evolution of standard deviation of the conductivity profiles (Sigma) along the helical and chaotic flow reactors for different Reynolds numbers.

L*/Lt is a nondimensional distance.

Table 3. Evolution of L^*/L_t According to Studied Reynolds Numbers for the Chaotic Flow Reactor and Helical Reactor

Re	L^*/L_t Chaotic Flow Reactor	L^*/L_t Helical Reactor
335	0.69	1.6
670	0.28	1.47
1005	0.2	1.17

port mechanism due to the action of Dean cells. The mixing efficiency enhancement with increasing Reynolds number cannot simply be explained by the decrease of the transit time in the reactor with increasing the Reynolds number. When omitting the effect of Dean cells, we estimate the time required to homogenize the solutions, by the sole effect of diffusion, in an area having the typical lengthscale of the pipe radius (10 mm) to be 50,000 s (for $D = 2\ 10^{-9}$ m^2/s). This timescale is much longer than the mixing timescale measured for the helical reactor. Interpreting the results of Table 3 in terms of time, we find the mixing time for $Re = 335$ to be $\tau^* = L^*/U = 918$ *s* in the chaotic flow reactor, whereas we extrapolate from Figure 9 that the mixing time would be 2127 s in the helical reactor. Dean cell's secondary flows also contribute to the process of diffusion in the helical reactor, although they do not change their orientation. By renewing the fluid at the interface which separates the two solutions, they contribute in speeding up the process of diffusion since they maintain steeper concentration gradients. This explains the reduction of the mixing time in the helical reactor when the Reynolds number is increased. The process of enhancement of the effective diffusivity across closed vortices was explained by Rhines and Young,[32] for the 2-D case of Rayleigh-Bénard cells and again considered by Young *et al.*[33] The existence of sustained diffusion boundary layers enhances the interfacial transport, as also observed in falling films, where interfacial waves can promote the transfer (Roberts and Chang[34]).

Mixing with chemical reaction

Figure 10 gives visual insight for a transversal concentration profile of triiodide and thisulfate concentrations obtained in the helical reactor downstream of bend 76 for $Re = 335$. The photograph shows the samples taken along the tube's diameter with a step of 2 mm, in which the remaining presence of triiodide (colored sample) or thiosulfate (transparent solution) is visible. The brown triiodide solution was sampled in the lower half of the tube and that of thiosulfate in the upper half of the tube. An indication of the concentration gradients, in that part of the tube where triiodide is present, is detectable from the change in color density.

Figure 11 compares the concentration profiles deduced from the dosage of samples of the two reagents at different positions along the two reactors for $Re = 335$. The dimensionless concentration plotted in Figure 11, is defined as the measured concentration divided by the initial concentration of a given reagent.

For the helical reactor, the concentration profiles are symmetrical with regard to the symmetry axis of the Dean cells (Ox axis). The minimum concentration of the two reagents is on the Ox axis, where the chemical reaction first occurs. The maximum concentration in the reagents is observed at the cores of the Dean cells where no chemical reaction is achieved. We additionally observe that the concentrations decrease at the tube walls because reagents contained in fluid particles that react on the Ox diameter of the tube are transported by the Dean cell's secondary flows along the wall of the tubular reactor, whereas particles along the wall are transported along the Ox axis where they can react. Similar observations on temperature profiles were made (Chagny et al.[35]) in a helical heat exchanger. The streamlines of the Dean cells secondary flows are barriers which reagents can cross only by the effect of molecular diffusion. As described for our passive mixing experiments, the process of diffusion enhanced in the boundary layers between the two Dean cells and along the tube wall is still active, but the disappearance of reagents and the appearance of products caused by the chemical reaction at the border of Dean cells (and eventually along the wall), also contribute to maintain the stepper concentration gradients of the reagents. A kind of "steady state" regime exists for the local gradients. However, the concentration profiles of reagents measured downstream of bend 76 for Re = 335 shows the chemical reaction is far from being completed at the outlet of the helical reactor. Significantly different observations are made in the chaotic flow reactor (Figure 11, right column). We first see that the symmetry of the curves is broken. A rapid evolution toward flat concentration profiles is clearly seen. This is obtained at the position of the 55th bend, which is the position where mixing was achieved for the same flow conditions in passive mixing experiments. The dimensionless concentration of each of the two reagents is almost reduced to zero when the 55th bend is reached since the reagents are injected initially in stoechiomet-

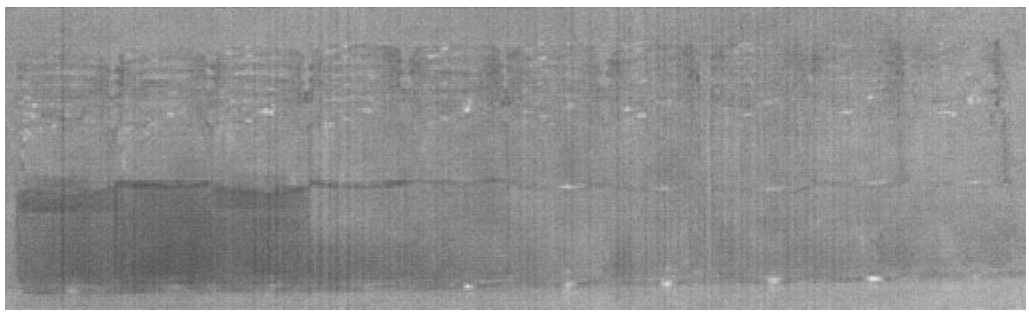

Figure 10. Samplings at the exit of the bend 76 for $Re = 335$ in the helical reactor.

The transversal positions of sampling are (from left to right): −0,9 cm; −0,7 cm; −0,5 cm; −0,3 cm; −0,1 cm; 0,1 cm; 0,3 cm; 0,5 cm; 0,7 cm; 0,9 cm in the Oy direction.

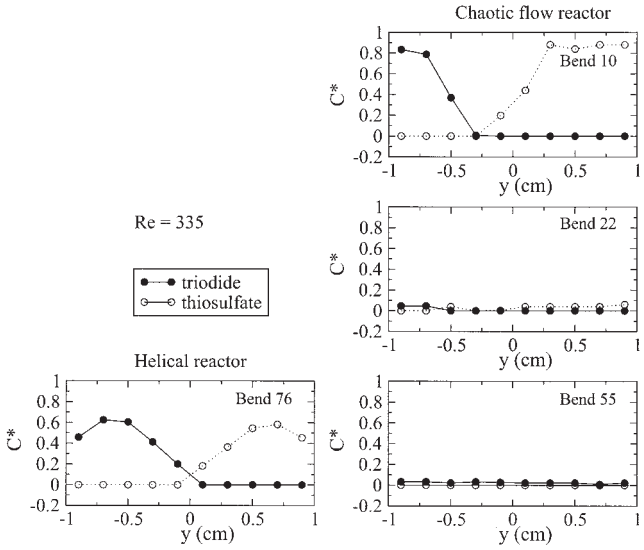

Figure 11. Dimensionless concentration profiles for each reagent in the two reactors for *Re* = 335.

ric proportion. The chaotic mixing, thus, generates a faster conversion of the reagents in the chaotic flow reactor as compared to the helical reactor. In the chaotic flow reactor, the reorientation of the Dean cells in each new bend modifies the concentration gradients in direction and intensity from one bend to the next, and induces the nonsymmetry of the reagents concentration profile observed at bend 10. In Figure 11, there is an indication of it.

Figure 12 shows the profiles of dimensionless concentrations of the two reagents in the two reactors for $Re = 670$. For the helical configuration, profiles similar to that obtained for $Re = 335$, are observed. The maximum concentrations are slightly lower than those measured for $Re = 335$, but the chemical conversion speed is only weakly increased by increasing the Reynolds number, as observed in passive mixing experiments (Table 3). In the chaotic flow reactor, the flatness of the concentration profiles is again observed at the same position as in passive mixing experiments.

Finally, Figure 13 presents the profiles of dimensionless

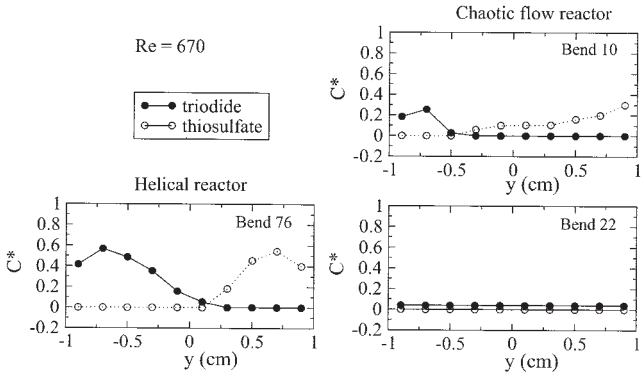

Figure 12. Dimensionless concentration profiles for each reagent in the two reactors for *Re* = 670.

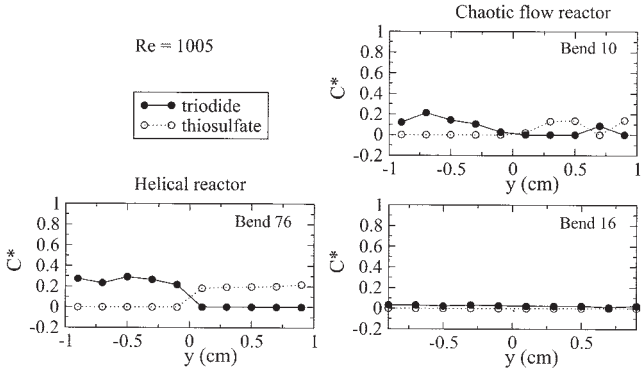

Figure 13. Dimensionless concentration profiles for each reagent in the two reactors for *Re* = 1005.

concentrations of reagents in the two reactors for a $Re = 1005$. For the helical configuration, one may no longer be able to distinguish the Dean cells, and a greater quantity of reagents is transformed. The flatness of the profiles indicates that we are approaching a flow with a potential core within each Dean cell, as is encountered in high Reynolds numbers in curved pipes. The increasing speed deforms the Dean's cells, and the instability of Dean can also appear to support the phenomenon of mixing. In the chaotic flow reactor, one observes a total transformation of the reagents at the end of 16 bends, as observed in passive mixing experiments.

Conclusion

In this article, we compared, in the laboratory, the diffusive and reactive mixing efficencies in two different coiled tubular reactors: a helical coil reactor and a twisted coiled reactor which is a chaotic flow reactor. A first observation is the similarity of the observations made for reactive and for passive mixing experiments.

On the basis of a criterion applied to the standard deviation of fluid conductivity measurements, taken along a pipe diameter, we estimated a mixing time for each reactor. In the helical reactor, the mixing by advection is considerably less effective than in the chaotic flow reactor and, therefore, the increase in the Reynolds number has less influence on the achievement of the mixing in the helical reactor, than in the chaotic flow reactor. In the chaotic flow reactor, the increase of inertial effects causes a decrease of the time required to reach a nearly perfect mixture. The mixing efficiency in the chaotic flow reactor is mainly explained by the rapid homogenization of "elementary volumes" of matter of various concentrations for neighboring streamlines. Stretching plays a key role as a direct consequence of the complex streamline patterns developed in the reactor. The reorientation (the folding) of the scalar filaments in each bend, stirs fluid elements of different concentrations, which are finally mixed by molecular diffusion.

Achieving a chemical reaction in the two reactors allowed to study mixing at a molecular scale, and to predict the contribution of the chaotic mixing on the conversion rate of the reagents, although the times measured to complete the reaction were not found to differ from the mixing times which were determined from passive mixing experiments. The major ob-

servation is the experimental proof that chemical conversion in the chaotic flow reactor is faster than obtained in the helical reactor. Despite the low spatial resolution of the samplings in a pipe cross-section, and due to the inherent complexity of experimental measurements in 3-D open flows, the efficiency of the mixing in the chaotic flow reactor for molecular scales has been proven. The chaotic flow configuration makes possible the reduction of the length of the reactor (especially when the Reynolds number is large), and this can be advantageous from a practical and economic viewpoint. This opens a promising avenue for future study with other types of chemical reaction. Another advantage of the chaotic flow configuration, not clarified here, but which was proven elsewhere (Castelain et al.[36]), is that it considerably tightens the distribution of residence times.

From a more practical point of view, one could advantageously plan to replace a helical tubular photobioreactor (Scragg et al.[37]) with a chaotic one of geometry similar to that studied here. The use of a chaotic flow reactor will facilitate access to light for the algae by assuring the renewal of all the fluid close to the tube wall. So, the time available for photosynthesis will be longer, and the reactor's length considerably reduced. The use of our chaotic flow reactor configuration could also be used as a microreactor (Liu et al.[38]; Yi and Bau[39]).

Comparing the chaotic flow reactor with another classical effective static mixing device (that is, the static mixer), we can first notice the considerably higher pressure drop reached within the static mixer. For a range of Reynolds numbers between 100 and 2,000, the friction factor ratio (as compared with the empty straight pipe) varies from 1.2 to 2.5 for the chaotic flow mixer (Castelain[40], Acharya et al.[5]) and from 1.5 to 2,000 for the static mixer (Fang and Lee[41]). Indeed, the chaotic flow reactor seems to be designed for an intermediate laminar regime (*Re* between 200 and 2,000) when high pressure drops or fouling problems occur in the static mixer. However, the length required to reach the same mixing level will be probably higher for the chaotic flow reactor, because the decrease of striation thickness is less controllable than in the static mixer. Szalai and Muzzio[42] have also recently shown in the static mixer that the intensity of mixing is not monotonically improved as the flow rate is increased. So, a careful study will be necessary to compare the chaotic flow reactor and static mixers in terms of chemical reaction advancement.

Some ideas can also be launched for new more fundamental studies. Recent studies (Voth et al.[43]) have shown that not only stretching distributions need to be considered to understand completely the mixing mechanism, but transport must also be considered. In our opinion, the twisted pipes chaotic flow reactor, with the presence of "trapping" and "ballistic" zones for the scalars constitutes a good prototype for promising future studies involving chaotic advection (stretching and folding) and reactive processes. For example, little attention has been devoted to studying folding field statistics to improve mixing; in comparison with all the studies related to stretching field statistics. Stretching refers only to the thinning of scalar filaments, whereas for homogenization, folding is necessary (via horseshoe transformation). Folding is more related to the curvature of streamlines, and is also more related to the presence of boundaries which induces differential residence times. Thus, the time delay between the actions of stretching and folding along a streamline is connected with transport. The interplay of these three mechanisms could constitute a new way of tackling the complex problem of chaotic mixing in reactive flows.

Literature Cited

1. Ottino JM. *The kinematics of Mixing: Stretching, Chaos and Transport*, Cambridge University Press; 1989.
2. Aref H. The development of chaotic advection. *Phys Fluids*. 2002; 14,1315-1325.
3. Peerhossaini H, Castelain C, Le Guer Y. Heat exchanger design based on chaotic advection. *Exp Therm and Fluid Sci.* 1993;7:333-344.
4. Mokrani A, Castelain C, Peerhossaini H. The effects of chaotic advection on heat transfer. *Int J Heat Mass Transfer*. 1997;40,13:3089-3104.
5. Acharya N, Sen M, Chang HC. Analysis of heat transfer enhancement in coiled-tube heat exchangers. *Int J Heat Mass Transfer*. 2001; 44,3189-3199.
6. Alvarez-Hernández MM, Shinbrot T, Zalc J, Muzzio FJ. Practical chaotic mixing. *Chem Eng Sci.* 2002;57,3749-3753.
7. Zumbrunnen DA, Inamdar S. Novel sub-micron highly multi-layered polymer films formed by continuous flow chaotic mixing. *Chem Eng Sci.* 2001;56:3893-3897.
8. Zumbrunnen DA, Chhibber C. Morphology development in polymer blends produced by chaotic mixing at various compositions. *Polymer*. 2002;43:3267-3277.
9. Kwon O, Zumbrunnen DA. Production of barrier films by chaotic mixing of plastics. *Polymer Eng and Sci.* 2003;43:1443-1459.
10. Ottino JM. Mixing and chemical reactions. A tutorial. *Chem Eng Sci*. 1994;49:4005-4027.
11. Metcalfe G, Ottino JM. Autocatalytic processes in mixing flows. *Phys Rev Letters*, 1994;72,18:2875-2878.
12. Neufeld Z, López C, Hernández-García E, Tél T. Multifractal structure of chaotically advected chemical fields. *Phys Rev E.* 2000;61:3857-3866.
13. Tél T, Károlyi G, Péntek A, Scheuring I, Torczkai Z, Grebogi C, Kadtke J. Chaotic advection, diffusion and reactions in open flows. *Chaos.* 2000;10,1:89-98.
14. Muzzio FJ, Liu M. Chemical reactions in chaotic flows. *Chem Eng J.* 1996;64:117-127.
15. Zalc JM, Muzzio FJ. Parallel-competitive reactions in a two dimensional chaotic flow. *Chem Eng Sci.* 1999;54:1053-1069.
16. Adrover A, Cerbelli S, Giona M. A spectral approach to reaction/diffusion kinetics in chaotic flows. *Comp and Chem Eng*. 2002;26,1: 125-139.
17. Bryden MD, Brenner H. Effect of laminar chaos on reaction and dispersion in eccentric annular flow. *J Fluid Mech.* 1996;325:219-237.
18. Tang XZ, Boozer AH. Design criteria of a chemical reactor based on a chaotic flow. *Chaos*. 1999;9:183-194.
19. Lamberto DJ, Muzzio FJ, Swanson PD, Tonkovitch AL. Using time-dependent RPM to enhance mixing in stirred vessels. *Chem Eng Sci.* 1996;51,5:733-741.
20. Szalai ES, Kukura J, Arratia, PE, Muzzio FJ. Effect of hydrodynamics on reactive mixing in laminar flows. *AIChE J.* 2003; 49, 1:168-179.
21. Sawyers DR, Sen M, Chang HC. Effect of chaotic interfacial stretching on bimolecular chemical reaction in helical-coil reactors. *The Chem Eng J.* 1996;64:129-139.
22. Paireau O, Tabeling P. Enhancement of the reactivity by chaotic mixing. *Phys Rev E*. 1997;56:2287-2290.
23. Le Guer Y, Peerhossaini H. Order breaking in Dean flow. *Phys Fluids A*. 1991;3,5:1029-1032.
24. Le Guer Y, Schall E. A mapping tool using anisotropic unstructured meshes to study mixing in periodic flows. *Chem Eng Sci.* 2004;59: 1459-1472.
25. Jones SW, Thomas OM, Aref H. Chaotic advection by laminar flow in a twisted pipe. *J Fluid Mech.* 1989;209:335-357.
26. Gibout S, Le Guer Y, Schall E. Coupling of a mapping method and a genetic algorithm to optimize mixing efficiency in periodic chaotic flow, submitted to *Comm Nonlin Sci Num Sim.* to be published in 2006 in *Comm Nonlin Sci Num Sim,* available online via Science Direct since Dec. 30, 2004.
27. Manning FS, Wilhelm RH. Concentration fluctuations in a stirred baffled vessel. *AIChE J.* 1963;9:12-19.

28. Gibson CH, Schwarz WH. Detection of conductivity fluctuations in a turbulent flow field. *J Fluid Mech.* 1963;16:357-364.
29. Boesinger C. *Mélange diffusif et réactif dans des réacteurs à trajectoires complexes*. France: Université de Pau et des Pays de l'Adour; 2002. PhD Thesis.
30. Scheper WM, Margerum DW. Non-metal redox kinetics: reactions of iodine and triiodine with thiosulfate via $I_2S_2O_3^{2-}$ and $IS_2O_3^-$ intermediates. *Inorg Chem*. 1992;31:5466-5473.
31. Lide D. *Handbook of Chemistry and Physics*. 84th ed. CRC Press; 2003.
32. Rhines PB, Young WR. How rapidly is a passive scalar mixed within closed streamlines? *J Fluid Mech*. 1983;133:133-145.
33. Young WR, Pumir A, Pomeau Y. Anomalous diffusion of tracer in convection rolls. *Phys Fluids*,.1989;A1:462-469.
34. Roberts RM, Chang HC. Wave-enhanced interfacial transfer. *Chem Eng Sci.* 2000;55:1127-1141.
35. Chagny C, Castelain C, Peerhossaini H. Chaotic heat transfer for heat exchanger design and comparison with a regular regime for a large range of Reynolds numbers. *Appl Therm Eng.* 2000;20:1615-1648.
36. Castelain C, Mokrani A, Le Guer Y, Peerhossaini H. Experimental study of chaotic advection regime in a twisted duct flow. *Eur J of Mechanics B/Fluids*. 2001;20:205-232.
37. Scragg AH, Illman AM, Carden A, Shales SW. Growth of microalgae with increased calorific values in a tubular biorector. *Biomass and Bioenergy*. 2002;23:67-73.
38. Liu RH, Stremler MA, Sharp KV, Olsen MG, Santiago JG, Adrian RJ, Aref H, Beebe DJ. Passive mixing in a three-dimensional serpentine microchannel. *J of Microelectromechanical Syst.* 2000;9:190-197.
39. Yi M, Bau HH. The kinematics of bend-induced mixing in microcircuits. *Int J of Heat and Fluid Flow*. 2003;24:645-656.
40. Castelain C. *Etude expérimentale de la dynamique des fluides et des transferts thermiques dans un écoulement de Dean alterné en régime d'advection chaotique*. France: Université de Nantes; 1995. PhD Thesis.
41. Fang JZ ,Lee DJ. Micromixing efficiency in static mixer. *Chem Eng Sci.* 2001;56:3797-3802.
42. Szalai ES, Muzzio FJ. Fundamental approach to the design and optimization of static mixers. *AIChE J*. 2003;49,11:2687-2699.
43. Voth GA, Saint T, Dobler G, Gollub JP. Mixing rates and symmetry breaking in two-dimensional chaotic flow. *Phys Fluids*. 2003;15:2560-2566.

Received Manuscript received Feb. 13, 2004; and revision received Nov. 8, 2004.